

## SUPPORTING INFORMATION

### Tuning Solvent Strength Can Fractionate PVC into Ultra-low Molecular Weight Material with Low Dispersity

Ali Al Alshaikh <sup>1</sup> (<https://orcid.org/0000-0002-5976-1176>)

Jaewoo Choi <sup>1</sup> (<https://orcid.org/0009-0009-3200-0842>)

Feranmi V. Olowookere <sup>1</sup> (<https://orcid.org/0009-0008-2110-2264>)

Caira McClairen <sup>2</sup> (<https://orcid.org/0009-0008-2262-761X>)

Owen Lubic <sup>1</sup> (<https://orcid.org/0009-0004-2485-0170>)

Pravin Shinde <sup>1</sup> (<https://orcid.org/0000-0002-1715-6867>)

C. Heath Turner <sup>1</sup> (<https://orcid.org/0000-0002-5707-9480>)

Jason E. Bara <sup>1\*</sup> (<https://orcid.org/0000-0002-8351-2145>)

<sup>1</sup> Department of Chemical & Biological Engineering, The University of Alabama, Tuscaloosa, AL USA  
35487-0203

<sup>2</sup> School of Chemical and Biomolecular Engineering, Georgia Institute of Technology, Atlanta, GA  
30332, USA

\*Corresponding author's email address: [jbara@eng.ua.edu](mailto:jbara@eng.ua.edu) (J. E. Bara)

## Table of Contents

<b>S1. Solvent-Based Recovery Literature Review.....</b>	<b>1</b>
<b>S2. Computational. ....</b>	<b>3</b>
S2.1. Computational Methods.....	3
S2.2. Computational Results.....	5
<b>S3. Additives. ....</b>	<b>7</b>
<b>S4. GPC Traces. ....</b>	<b>9</b>
<b>S5. FTIR Spectra.....</b>	<b>12</b>
<b>S6. DSC Scans. ....</b>	<b>13</b>
<b>S7. Other. ....</b>	<b>15</b>
<b>REFERENCES FOR SUPPORTING INFORMATION .....</b>	<b>17</b>

## List of Figures

<b>Fig. S 1 (a)</b> Volume of mixing ( $\text{cm}^3/\text{kg}$ ) and <b>(b)</b> Flory-Huggins interaction parameter $\chi_{12}$ for PVC in Ace-MeOH and THF-MeOH mixes at different MeOH % and at different $n_{\text{PVC}}$ .....	7
<b>Fig. S 2</b> Hansen Solubility Parameter (HSP) Distance $R_a$ ( $\text{MPa}^{1/2}$ ) between PVC and Ace-MeOH and THF-MeOH mixtures at different % MeOH. ....	7
<b>Fig. S 3</b> Photograph of PVC pipe trimmings (left) and PVC pellets (right).....	8
<b>Fig. S 4</b> GPC traces of PVC K-50 single-step fractionation products.....	9
<b>Fig. S 5</b> GPC traces of PVC K-50 sequential fractionation products.....	9
<b>Fig. S 6</b> GPC traces of Commercial PVC sequential fractionation products. ....	10
<b>Fig. S 7</b> GPC traces of PVC K-65, and the product of single-step 100% Ace fractionation (F65).....	10
<b>Figure S 8.</b> GPC traces of extracts of <b>(a)</b> 50% PVC K-50 and 50% PVC K-65 <b>(b)</b> 80% PVC K-50 and 20% PVC K-65 <b>(c)</b> 20% PVC K-50 and 80% PVC K-65. ....	11
<b>Figure S 9.</b> GPC traces of blended <b>(a)</b> PVC K-50 and K-65, <b>(b)</b> C3 and K-65, <b>(c)</b> C7 and K-50, <b>(d)</b> C8 and K-50.....	11
<b>Fig. S 10</b> FTIR spectra of PVC pipe, and PVC pipe cleaned via dissolution, centrifuge and precipitation. ....	12
<b>Fig. S 11</b> FTIR spectra of PVC pellet, plasticizer (DINP) extracted by soaking PVC pellets in a 60% Ace – 40% MeOH solvent mixture, and PVC pellet cleaned via dissolution, centrifuge and precipitation.....	12
<b>Fig. S 12</b> FTIR spectra of PVC K-65, and the product of single-step 100% Ace fractionation (F65).....	13
<b>Fig. S 13</b> DSC scans of PVC K-50 single-step fractionation products. ....	13
<b>Fig. S 14</b> DSC scans of PVC K-50 sequential fractionation products.....	14
<b>Fig. S 15</b> DSC scans of commercial PVC sequential fractionation products.....	14
<b>Fig. S 16</b> DSC scans of PVC K-65, and the product of single-step 100% Ace fractionation (F65). ....	15
<b>Fig. S 17</b> Solution dynamic viscosity ( $\mu$ ) of acetone fractions of PVC K-50 and K-65. Solution concentration: 100 mg PVC per 1 mL solvent (THF). ....	15

## List of Tables

<b>Table S 1.</b> Literature review of recent solvent-based recovery of plastics. ....	1
<b>Table S 2.</b> Summary of the simulated system compositions.....	3
<b>Table S 3.</b> Density of PVC-Ace-MeOH and PVC-THF-MeOH systems with different $n_{\text{PVC}}$ corresponding to Table S2, as well as $R_g$ values of the PVC in these systems. ....	6
<b>Table S 4.</b> Summary of single-step fractionation experiments of blended PVC resins. ....	16
<b>Table S 5.</b> Summary of blended PVC molecular weight data.....	16

## S1. Solvent-Based Recovery Literature Review.

**Table S 1.** Literature review of recent solvent-based recovery of plastics.

Material	Plastic	Solvent/Recovery <sup>a</sup>	Purity	Yield	Methods <sup>b</sup>	Ref
Flexible metalized packaging waste	PE	Biodiesel, 2-MeTHF, CPME / filtration + EtOH (biodiesel), evaporation (other solvents)	No figure given. Similar thermal and mechanical properties to original polymer	100%	Product was dissolved in solvent, then aluminum was removed by filtration while solution was hot. Aluminum fraction underwent another dissolution for full recovery of PE.	1
Multilayer plastic film	1: PE / EVOH / PET / EVA 2: PETG / PE / EVOH / PET / EVA	1: TOL (PE), DMSO (EVOH) / Ace (PE), H <sub>2</sub> O (EVOH), filtration (PET) 2: DMF-40% THF (PETG), TOL (PE, EVA), DMSO-40% water (EVOH) / PrOH (PETG), Cooling solvent followed by filtration (PE, EVOH), Ace (EVA), filtration (PET)	No figure given. Showed comparable properties to virgin resins. IR showed minor residual (other) polymer in some cases.	100%	Solvent-Targeted Recovery And Precipitation (STRAP) <sup>2</sup>	3
Multilayer plastic film	PE / EVOH / PET / PU ink	Dodecane (PE), DMSO-40% H <sub>2</sub> O (EVOH), GVL (PU ink) / Cooling solvent followed by filtration (PE, EVOH), filtration of GVL+PU (PET)	No figure given. Showed comparable properties to virgin resins. Some differences in crystallinity.	Overall Mass balance > 95%	Solvent-Targeted Recovery And Precipitation (STRAP) <sup>2</sup>	4
Face mask	PP	TOL (extraction), DMAc (decoloration) / Cooling solvent followed by filtration	No figure given. Similar thermochemical properties and color to virgin PP resin.	Up to 73.53%	Solvent-Targeted Recovery And Precipitation (STRAP) <sup>2</sup>	5
Face mask	PP	p-cymene / EtOH, ethylene sulfite, GVL, terpineol	No figure given. Same chemical properties as standard PP.	Up to 94%	Dissolution/precipitation.	6
Post-consumer white expanded polystyrene	PS	p-cymene / heptane	No figure given. Showed similar $M_w$ and $M_n$ to initial polymer.	NA	Study compares mechanical recycling to solvent based recovery. 4 cycles of dissolution followed by filtration, centrifuge, and precipitation.	7
Waste packaging materials	PS	essential oils / MeOH, IPA	No figure given. No chemical changes during recovery	Up to 80%	Dissolution/precipitation.	8

*Continued on Next Page*

Table S1. Continued.

Material	Plastic	Solvent/Recovery <sup>a</sup>	Purity	Yield	Methods <sup>b</sup>	Ref
waste packaging	PS	Omega-3, Tributyrin and ethyl butyrate / MeOH, IPA	No figure given. Did not undergo structural changes during recovery.	NA	Dissolution/precipitation.	<sup>9</sup>
Waste water bottles	PET	TCE / MeOH	No figure given. Recycled PET sowed kinetics were consistent with reported data on pure PET.	NA	Dissolution/precipitation.	<sup>10</sup>
Reverse osmosis membranes	PA / PSf / PET	DMF / H <sub>2</sub> O (PSf recovery)	No figure given. PET and PSf showed similar structures and properties to commercially available polymers. PA recovered was cross-linked and had PSf content.	NA	PET recovered by delamination of layered membrane in DMF. Polysulfone dissolved in DMF and was recovered by precipitation in water. Chlorine treatment was used to remove residual polyamide in polysulfone.	<sup>11</sup>
Textile waste	Polyester	N, N-dimethylcyclohexylamine / H <sub>2</sub> O	No figure given. Shows similar results to previously reported pure and treated polyester.	96%	Switchable hydrophilicity solvent was used. Textile dye is first leached using HNO <sub>3</sub> , then polyester dissolved separating it from cotton fiber.	<sup>12</sup>
Waste PA6/spandex	PU / Nylon 6	DMF / H <sub>2</sub> O	No figure given. Shows similar structure and properties to virgin resin.	NA	PU stripped from PU/PA6 blend.	<sup>13</sup>
e-waste	PC	NMP / H <sub>2</sub> O   DCM / MeOH	No figure given. Flame retardant (phosphorus-containing) removed by 30%. Product degraded through hydrolysis.	90%	PC was separated using density separation (sink/float).	<sup>14</sup>
Flame Retardant PC/ABS resin	PC / ABS copolymer	N, N-dimethylcyclohexylamine / filtration	No figure given. Phosphorus content reduced to almost zero. High purity resin, and additive recovered.	Up to 94%	Switchable hydrophilicity solvent was used.	<sup>15</sup>

Continued on Next Page

Table S1. Continued.

Material	Plastic	Solvent/Recovery <sup>a</sup>	Purity	Yield	Methods <sup>b</sup>	Ref
Vinyl-coated fabric	PVC / PET	THF, MEK, DMF, Cyclopentanone, Cyclohexanone / evaporation	No figure given. DMF and MEK did not remove all PVC from PET.	Up to complete dissolution.	Solvent selection study. PVC removed by dissolution from fibers.	<sup>16</sup>

**Polymer Nomenclature:** PE = Polyethylene; EVOH = Ethylene vinyl alcohol; PET = Polyethylene terephthalate; EVA = Ethylene-vinyl acetate; PETG = polyethylene terephthalate glycol-modified; PU = Polyurethane; PS = Polystyrene; PA = Polyamide; PSf = Polysulfone; PC = Polycarbonate; ABS = Acrylonitrile butadiene styrene; PVC = Polyvinyl chloride.

**Solvent Nomenclature:** 2-MeTHF = 2-Methyltetrahydrofuran; CPME = Cyclopentyl methyl ether; EtOH = Ethanol; TOL = Toluene; DMSO = Dimethyl sulfoxide; Ace = Acetone; H<sub>2</sub>O = Water; THF = Tetrahydrofuran; PrOH = 1-Propanol; GVL =  $\gamma$ -Valerolactone; DMAc = N,N-dimethylacetamide; MeOH = Methanol; IPA = Isopropyl alcohol (2-propanol); Omega-3 = Ethyl ester fish oil; Tributyrin = Glyceryl tributyrate; TCE = 1,1,2,2-tetrachloroethane; DMF = Dimethylformamide; NMP = N-methylpyrrolidone; DCM = Dichloromethane; MEK = Methyl ethyl ketone (2-butanone)

<sup>a</sup> Anti-solvent used, or recovery method if no solvent was used.

<sup>b</sup> Details indicated here only when deemed necessary. In most cases, methods involved dissolution and recovery through precipitation.

## S2. Computational.

### S2.1. Computational Methods.

Table S 2. Summary of the simulated system compositions.

No. of PVC <sub>120</sub> chains ( $n_{PVC}$ )	MeOH %	Number of molecules present			
		Ace-MeOH		THF-MeOH	
		Ace	MeOH	THF	MeOH
5	0	1378	0	1109	0
5	20	1102	499	886	499
5	40	826	999	664	999
5	60	551	1499	443	1499
5	80	276	1999	222	1999
10	0	1378	0	1109	0
10	20	1102	499	886	499
10	40	826	999	664	999
10	60	551	1499	443	1499
10	80	276	1999	222	1999
15	0	1378	0	1109	0
15	20	1102	499	886	499
15	40	826	999	664	999
15	60	551	1499	443	1499

Surface area (SA) values of the PVC molecules were obtained using the Gromacs tool *gmx sasa*, while the PVC radius of gyration ( $R_g$ ) was calculated using the Plumed package.<sup>17</sup> The Flory-Huggins (FH) interaction parameter  $\chi_{12}$  was determined following our previous protocol,<sup>18</sup> based on the Flory-Huggins solution theory:<sup>19</sup>

$$\chi_{12} = \frac{H^E}{RTN_1\Phi_2} \quad (\text{Eq. S1})$$

where  $H^E$  is the enthalpy of mixing,  $R$  is the universal gas constant,  $T$  is the temperature,  $N_1$  is the number of solvent molecules,  $\Phi_2$  is the lattice volume fraction  $\Phi_2 = \frac{xN_2}{N}$ ,  $N_2$  is the number of PVC<sub>120</sub> chains, each of which has  $x$  repeat units, and  $N$  is the total number of sites ( $N = N_1 + xN_2$ ). To calculate  $H^E$ , we simulated PVC-solvent mixtures, individual solvents (Ace, THF, MeOH) and bulk PVC systems and used the following equation:

$$H^E = \langle H \rangle_m - \sum x_i \langle H \rangle_i \quad (\text{Eq. S2})$$

where  $\langle H \rangle_m$  is the ensemble average molar enthalpy of the mixture (with 1 mol of PVC corresponding to a PVC<sub>120</sub> chain), and  $x_i$ ,  $\langle H \rangle_i$  and  $\langle V \rangle_i$  represent the mole fraction, enthalpy, and molar volume of  $i$ th compound in its liquid state, respectively. The volume of mixing ( $V^E$ ) can be similarly obtained through Eq. S3:

$$V^E = \langle V \rangle_m - \sum x_i \langle V \rangle_i \quad (\text{Eq. S3})$$

where  $\langle V \rangle_m$  represent the ensemble average molar volume of the mixture.

The Hansen solubility parameter ( $\delta_{Hans}$ ) is calculated as the square root of the cohesive energy density (CED), expressed as the sum of contributions from different interactions:<sup>20</sup>

$$\delta_{Hans}^2 = \delta_d^2 + \delta_p^2 + \delta_h^2 \quad (\text{Eq. S4})$$

where  $\delta_d$ ,  $\delta_p$ , and  $\delta_h$  represent the dispersion (van der Waals), polar (dipole-dipole), and hydrogen bonding interactions, respectively. Since the OPLS-AA force field does not include an explicit hydrogen bond term, the polar and hydrogen bonding contributions cannot be separated. Therefore,  $\delta_p$  and  $\delta_h$  are combined into a single electrostatic term  $\delta_e$ , similar to Salehi et. al's work:<sup>21</sup>

$$\delta_e^2 = \delta_p^2 + \delta_h^2 \quad (\text{Eq. S5})$$

The HSP of the Ace-MeOH and THF-MeOH mixtures (in MPa<sup>1/2</sup>) was calculated using the average potential energy of the liquid phase and gas phases as:

$$\delta_k^2 = \frac{\left( x_1 \cdot \left\langle \sum_i^n E_{k,gas}^{ACE} - E_{k,liq}^{ACE} \right\rangle + x_2 \cdot \left\langle \sum_i^n E_{gas}^{MeOH} - E_{liq}^{MeOH} \right\rangle \right)}{\langle V_m \rangle} \quad (\text{Eq. S6})$$

where  $k$  represents the Hansen components ( $k$  = dispersion and electrostatic),  $\langle \dots \rangle$  denotes a time-averaged ensemble,  $V_m$  is the molar volume of the mixture in cm<sup>3</sup>/mol,  $E_{k,gas}$  and  $E_{k,liq}$  are the gas and liquid phase energies of the components (J/mol),  $x_1$  and  $x_2$  represent the molar fractions of Ace/THF and MeOH, respectively. For bulk PVC, the MeOH contribution is zero:

$$\delta_k^2 = \frac{\left\langle \sum_i^n E_{k,gas}^{PVC} - E_{k,liq}^{PVC} \right\rangle}{\langle V_m \rangle} \quad (\text{Eq. S7})$$

The liquid phase simulations were performed in the NPT ensemble (averaged from three independent runs) using the aforementioned protocol for 50 ns, sampled every 10 ps. Gas phase simulations were run in the NVT ensemble for isolated Ace, THF, and MeOH molecules in a 100 Å box to minimize periodic boundary conditions (PBC) effects. After 200 ps of equilibration (timestep = 0.1 fs), average energy values were taken from a 1 ns production run. These energies were used to calculate the HSP components and total HSP in Eq. S8.

Finally, the HSP Distance  $Ra$  between PVC and the mixtures (Ace-MeOH and THF-MeOH) was calculated to assess their compatibility in solubility space. A smaller  $Ra$  indicates higher compatibility between components. The equation is:

$$Ra^2 = 4(\delta_{D1} - \delta_{D2})^2 + (\delta_{E1} - \delta_{E2})^2 \quad (\text{Eq. S8})$$

where  $\delta_{D1}$  and  $\delta_{D2}$  are dispersion terms of PVC and solvent mixture, respectively, and  $\delta_{E1}$  and  $\delta_{E2}$  are the electrostatic terms of PVC and solvent mixture, respectively.

## S2.2. Computational Results.

Table S3 shows that the density decreases with increasing MeOH concentrations in both PVC-Ace-MeOH and PVC-THF-MeOH mixtures. As expected, increasing  $n_{PVC}$  results in increased density due to the higher

PVC concentration. Given the high PVC concentration in this study, direct comparison of density with experiments may be challenging. However, our previous work<sup>22</sup> using the same force field parameters and models showed excellent agreement with experimental density values.

**Table S 3.** Density of PVC-Ace-MeOH and PVC-THF-MeOH systems with different  $n_{PVC}$  corresponding to Table S2, as well as  $R_g$  values of the PVC in these systems.

No. of PVC <sub>120</sub> chains ( $n_{PVC}$ )	MeOH %	Density of PVC-Ace-MeOH (g/cm <sup>3</sup> )	Density of PVC-THF-MeOH (g/cm <sup>3</sup> )	$R_g$ of PVC in Ace-MeOH (nm)	$R_g$ of PVC in THF-MeOH (nm)
5	0	0.952	1.003	2.22 ± 0.04	2.76 ± 0.07
5	20	0.939	0.984	2.07 ± 0.04	2.64 ± 0.07
5	40	0.937	0.970	1.63 ± 0.06	2.44 ± 0.04
5	60	0.936	0.957	1.38 ± 0.05	2.10 ± 0.05
5	80	0.932	0.946	1.35 ± 0.02	1.57 ± 0.03
10	0	1.037	1.091	2.05 ± 0.01	2.61 ± 0.02
10	20	1.032	1.073	1.87 ± 0.01	2.34 ± 0.02
10	40	1.029	1.060	1.83 ± 0.04	2.22 ± 0.03
10	60	1.030	1.048	1.73 ± 0.03	2.04 ± 0.01
10	80	1.022	1.036	1.55 ± 0.04	2.05 ± 0.04
15	0	1.101	1.150	1.63 ± 0.02	2.55 ± 0.03
15	20	1.097	1.134	1.54 ± 0.03	2.48 ± 0.02
15	40	1.093	1.122	1.48 ± 0.03	2.21 ± 0.03
15	60	1.089	1.109	1.46 ± 0.01	2.20 ± 0.01
15	80	1.085	1.097	1.46 ± 0.01	2.18 ± 0.02

We calculated the  $V^E$  and  $H^E$  and used the latter to determine the Flory-Huggins (FH) interaction parameters shown in Fig. S1. For all  $n_{PVC}$  in both mixtures,  $V^E$  (Fig. S1(a)) becomes less negative as % MeOH increases. Higher  $n_{PVC}$  shows more negative  $V^E$ , indicating stronger contraction during mixing in both mixtures. The Ace-MeOH mixture exhibits stronger contraction (more negative  $V^E$ ) compared to the THF-MeOH mixture, particularly at low MeOH concentrations. However, the difference narrows as % MeOH increases.

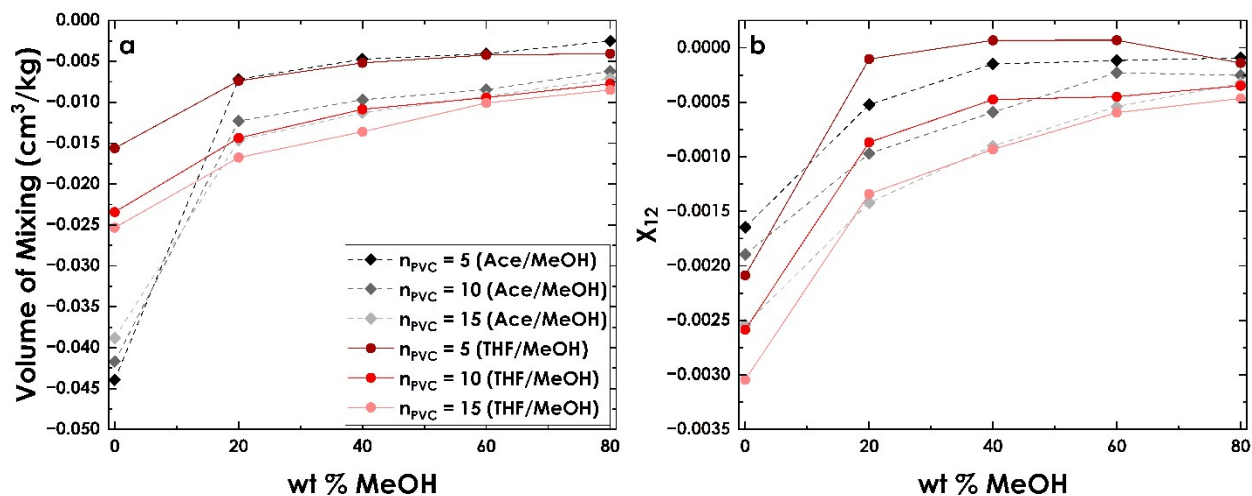


**Fig. S 1 (a)** Volume of mixing ( $\text{cm}^3/\text{kg}$ ) and **(b)** Flory-Huggins interaction parameter  $\chi_{12}$  for PVC in Ace-MeOH and THF-MeOH mixes at different MeOH % and at different  $n_{PVC}$ .

In Fig. S1(b), the less negative  $\chi_{12}$  with increasing % MeOH suggests reduced PVC-solvent interactions in both mixtures. In other words, MeOH acts as an anti-solvent, weakening polymer-solvent interactions and enabling the fractional precipitation of different MW fractions of PVC. Lower  $n_{PVC}$  has weaker polymer-solvent interactions, reflected by the less negative  $\chi_{12}$  values. In contrast, higher  $n_{PVC}$  shows a more negative  $\chi_{12}$ , indicating stronger enthalpic polymer-solvent interactions. Although this may seem counterintuitive, the increased number of PVC chains leads to more entanglement and fewer free chain ends, resulting in stronger solvent interactions per unit of PVC.

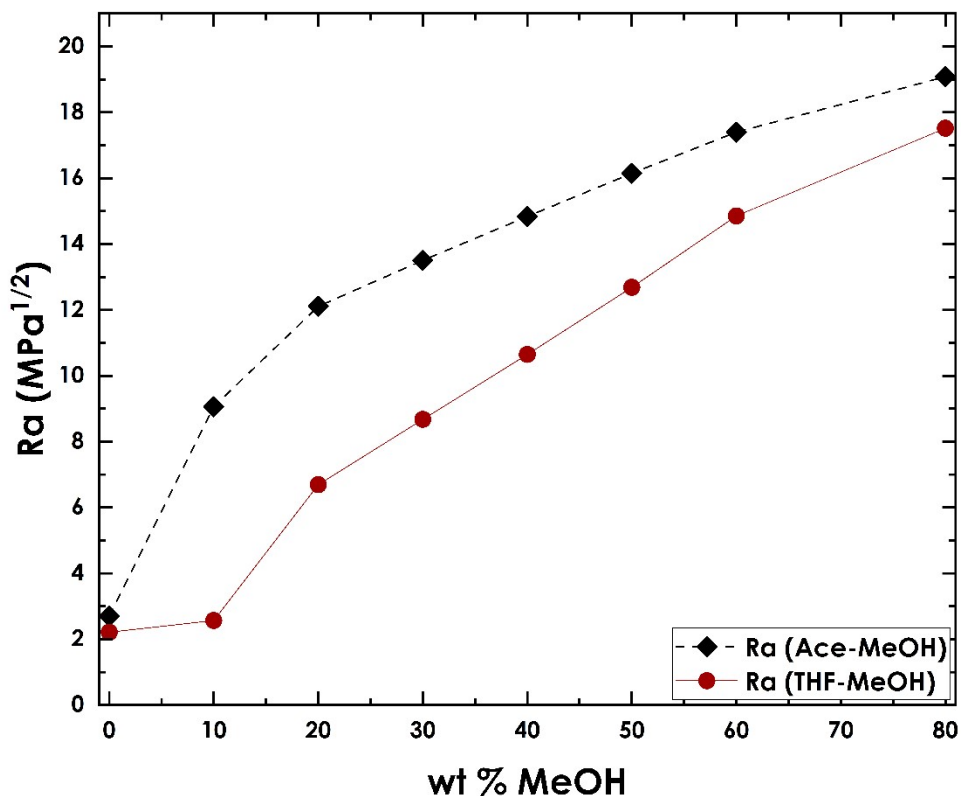


**Fig. S 2** Hansen Solubility Parameter (HSP) Distance  $R_a$  ( $\text{MPa}^{1/2}$ ) between PVC and Ace-MeOH and THF-MeOH mixtures at different % MeOH.

### S3. Additives.

PVC pellets and pipe (Fig. S3) used in this work contained significant additive content by mass. Through dissolution, filtration and precipitation, it was found that PVC pipe contained roughly 14% additives by mass which reasonably aligns with information on typical pipe formulations<sup>23</sup>. Determination of the exact identities and weight fractions of additives in pipe (wherein  $\text{CaCO}_3$  is expected to be the primary non-PVC component) is complicated and not necessary for the goals of this work. PVC pipe is expected to contain mostly inorganic stabilizers and fillers that are easily removed via centrifuge or filtration when PVC is dissolved in a suitable solvent (Fig. S8). PVC pellet had a much larger additive content, ~29% by mass, but likely slightly larger as some residual additive can be seen in some fractionation products, albeit at low concentrations. The plasticizer used in PVC pellet was determined previously to be di-isononyl

terephthalate (DINT)<sup>24</sup> (Fig. S9). Nonetheless, simply through dissolution, centrifuge/filtration and precipitation in hexane, followed by a MeOH wash, PVC pellets can be cleaned thoroughly (Fig. S9).

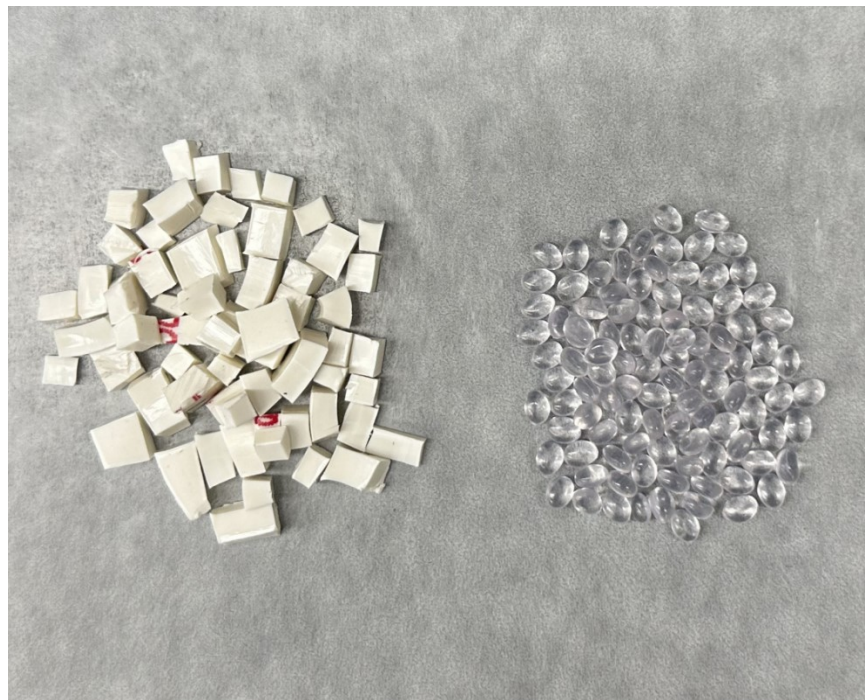


**Fig. S 3** Photograph of PVC pipe trimmings (left) and PVC pellets (right).

S4. GPC Traces.

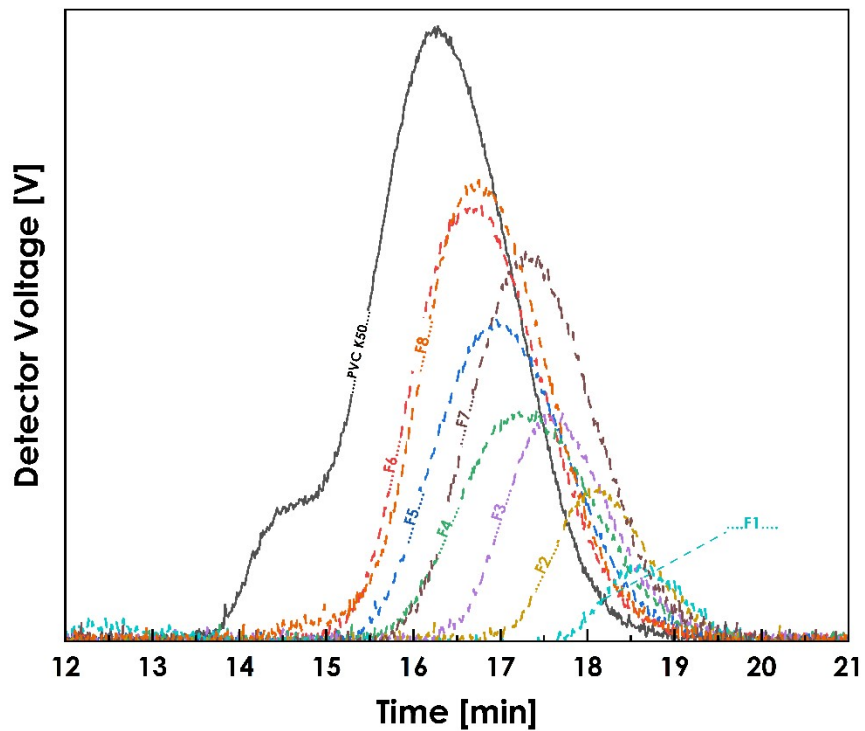


Fig. S 4 GPC traces of PVC K-50 single-step fractionation products.

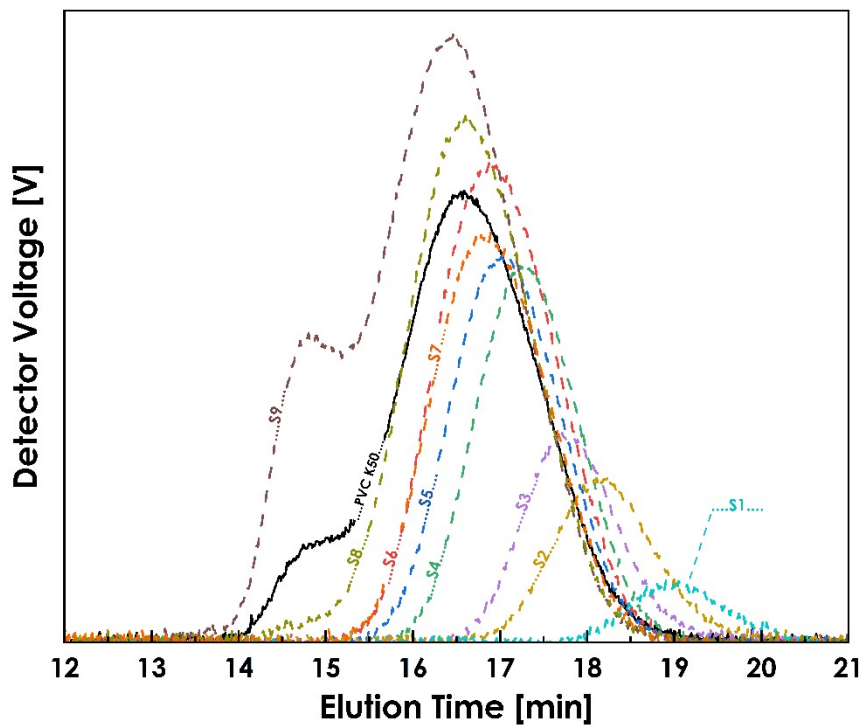


Fig. S 5 GPC traces of PVC K-50 sequential fractionation products.

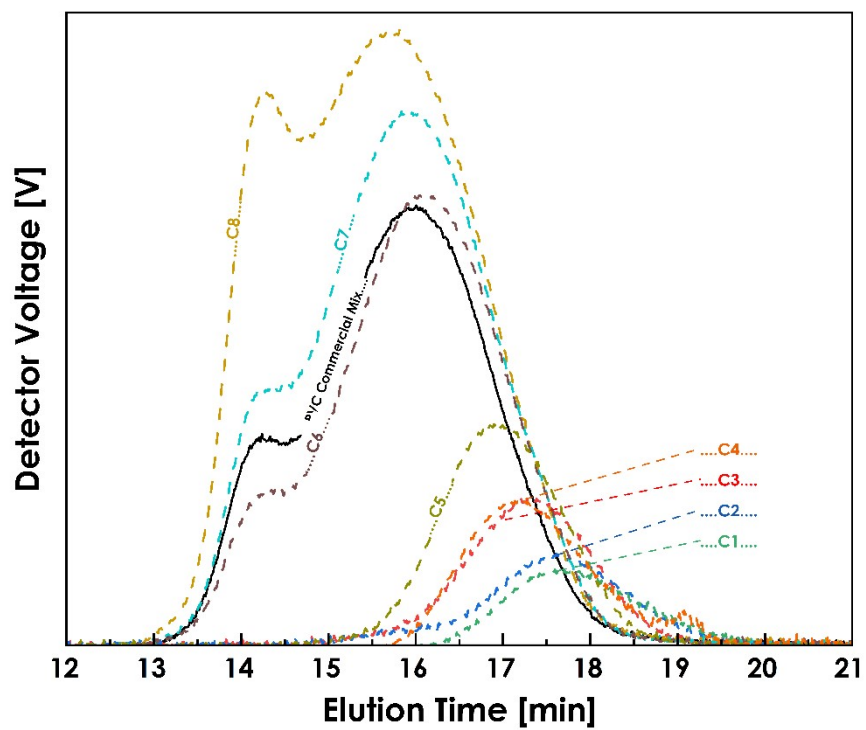


Fig. S 6 GPC traces of Commercial PVC sequential fractionation products.

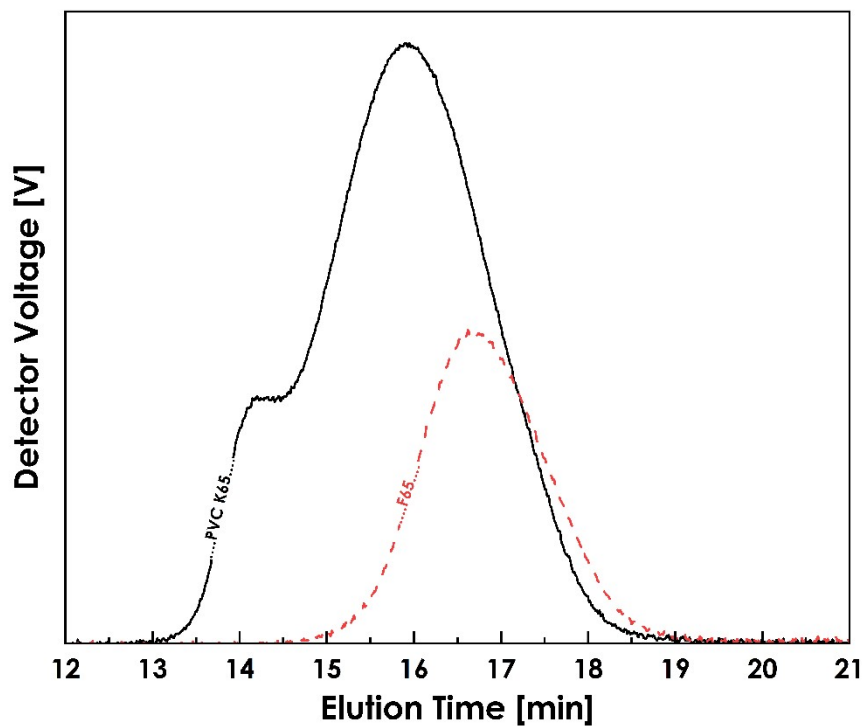
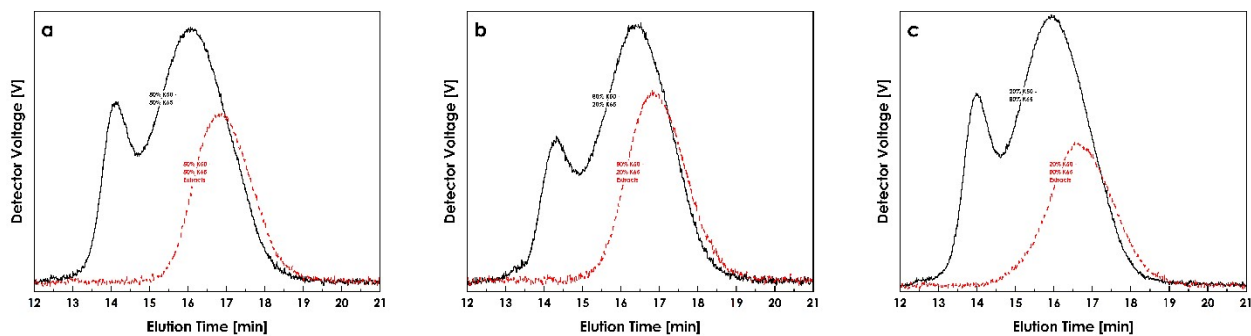
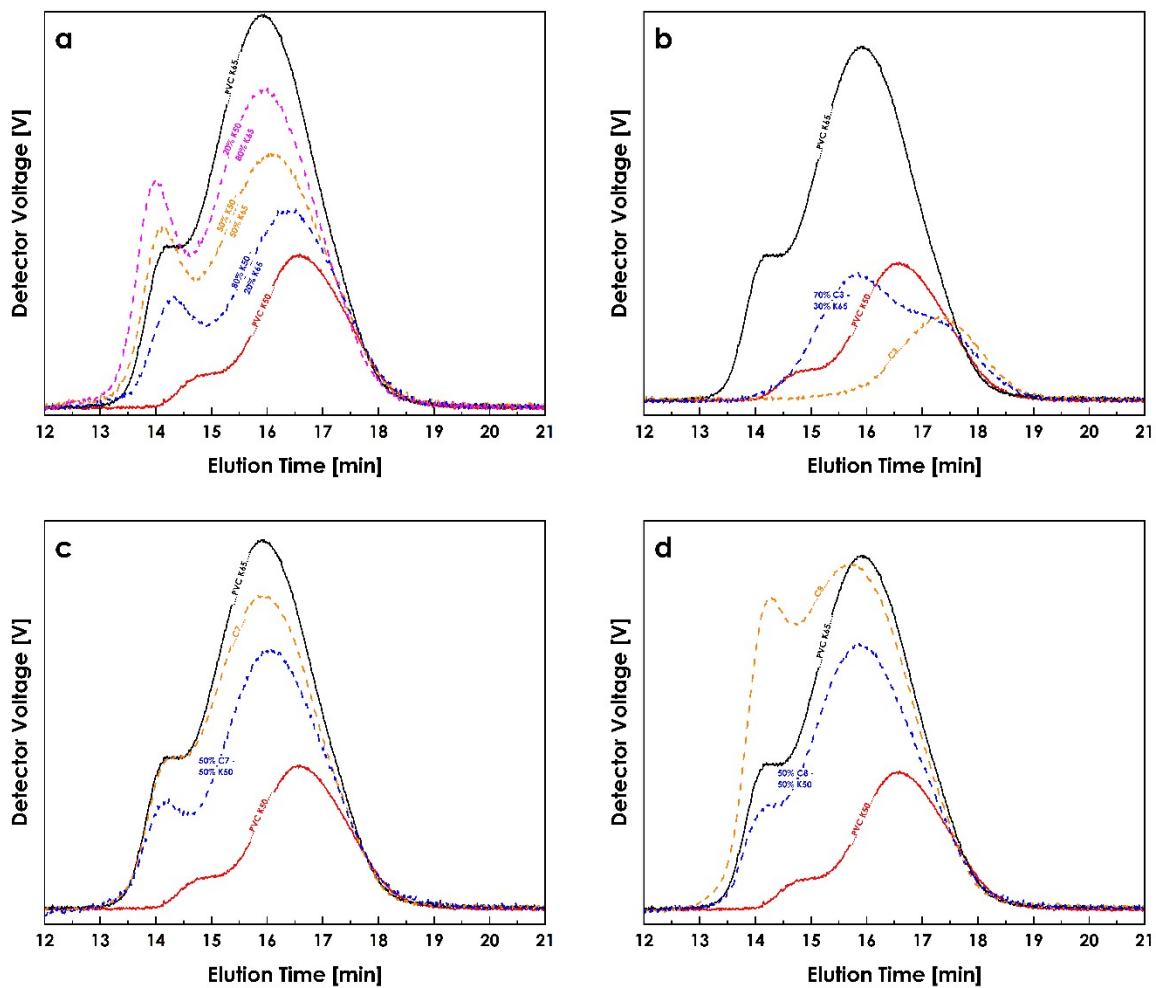


Fig. S 7 GPC traces of PVC K-65, and the product of single-step 100% Ace fractionation (F65).



**Figure S 8.** GPC traces of extracts of (a) 50% PVC K-50 and 50% PVC K-65 (b) 80% PVC K-50 and 20% PVC K-65 (c) 20% PVC K-50 and 80% PVC K-65.



**Figure S 9.** GPC traces of blended (a) PVC K-50 and K-65, (b) C3 and K-65, (c) C7 and K-50, (d) C8 and K-50.

## S5. FTIR Spectra

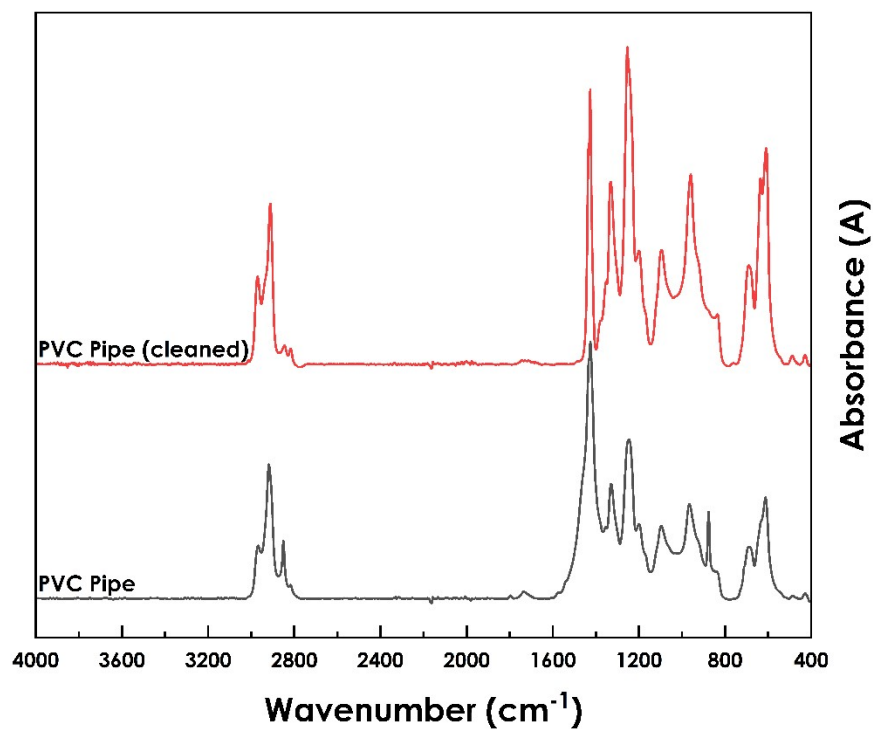


Fig. S 10 FTIR spectra of PVC pipe, and PVC pipe cleaned via dissolution, centrifuge and precipitation.

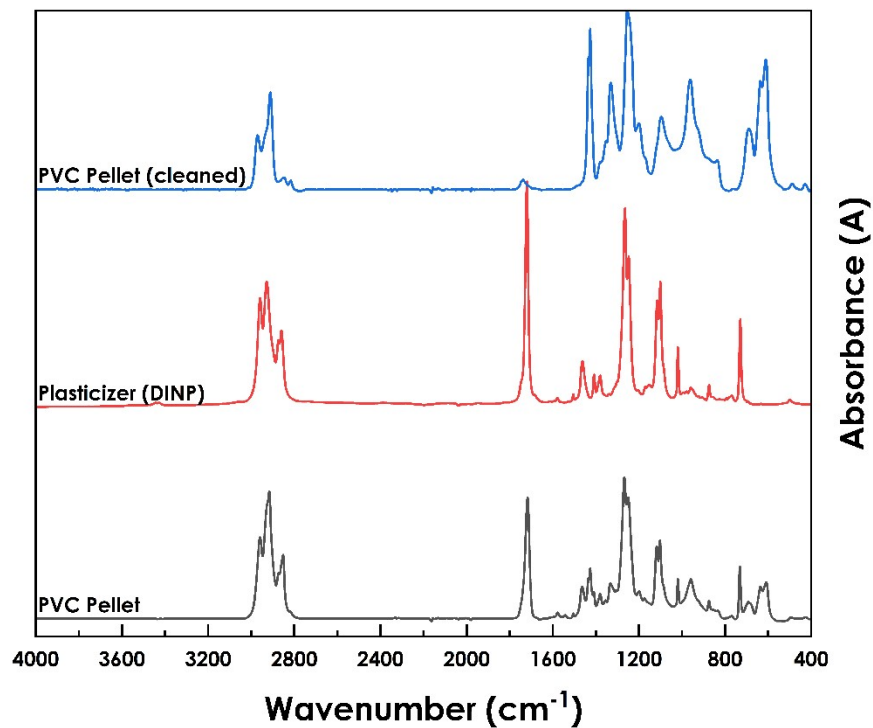


Fig. S 11 FTIR spectra of PVC pellet, plasticizer (DINP) extracted by soaking PVC pellets in a 60% Ace – 40% MeOH solvent mixture, and PVC pellet cleaned via dissolution, centrifuge and precipitation.

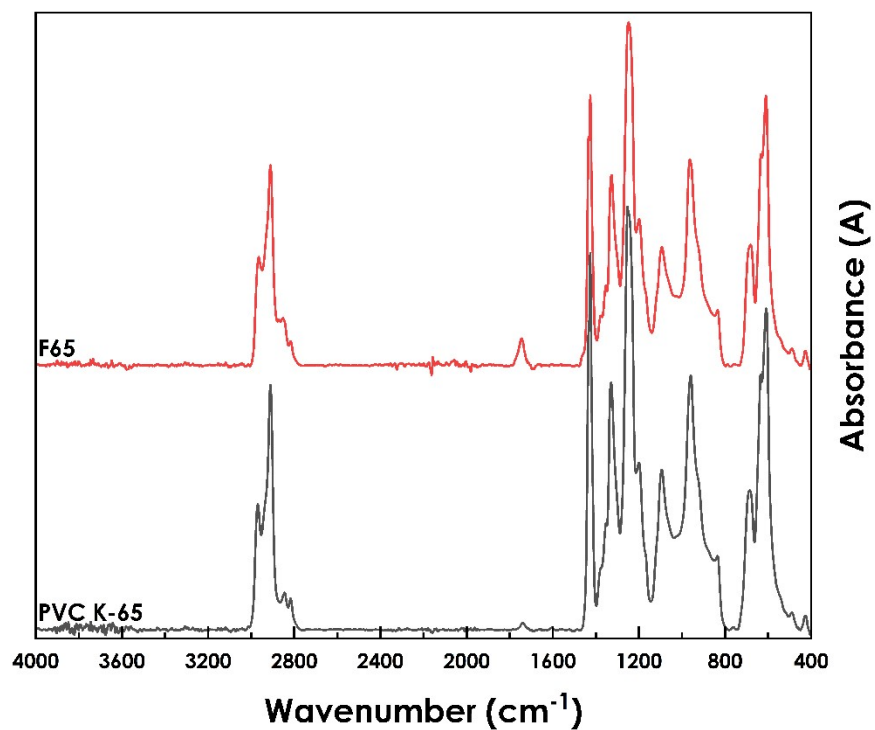


Fig. S 12 FTIR spectra of PVC K-65, and the product of single-step 100% Ace fractionation (F65).

S6. DSC Scans.

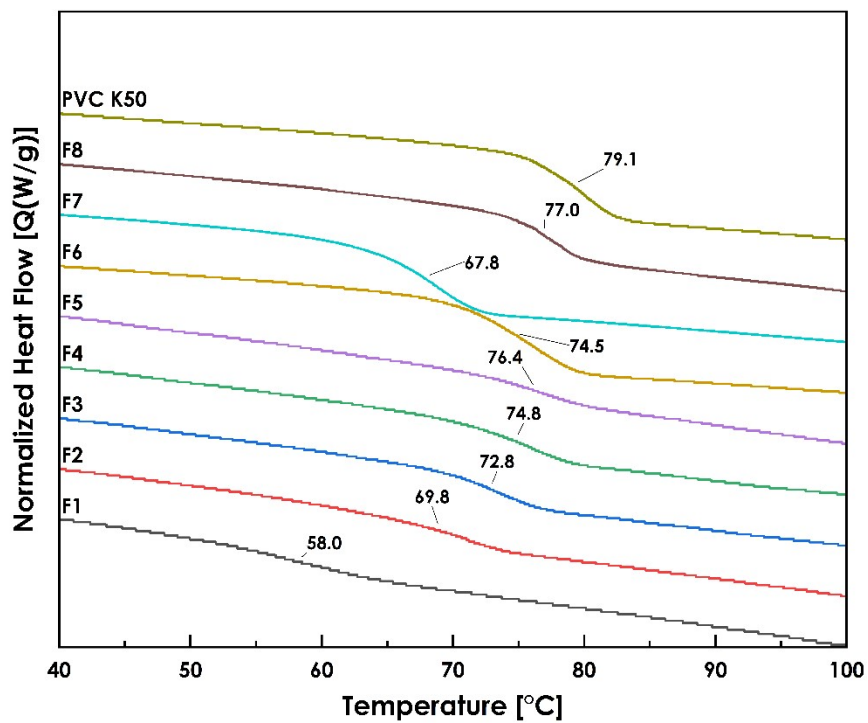


Fig. S 13 DSC scans of PVC K-50 single-step fractionation products.

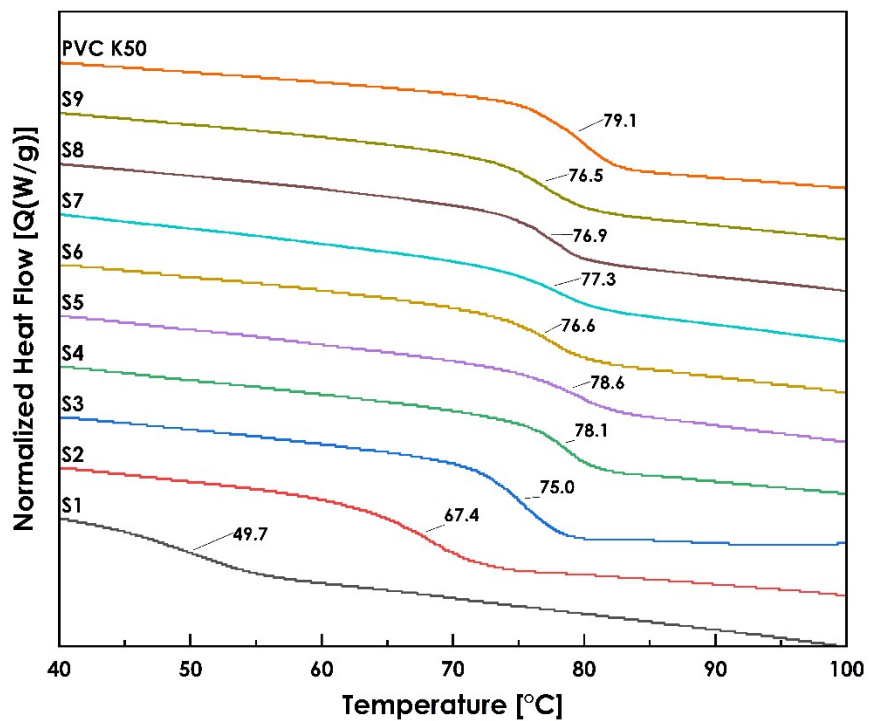


Fig. S 14 DSC scans of PVC K-50 sequential fractionation products.

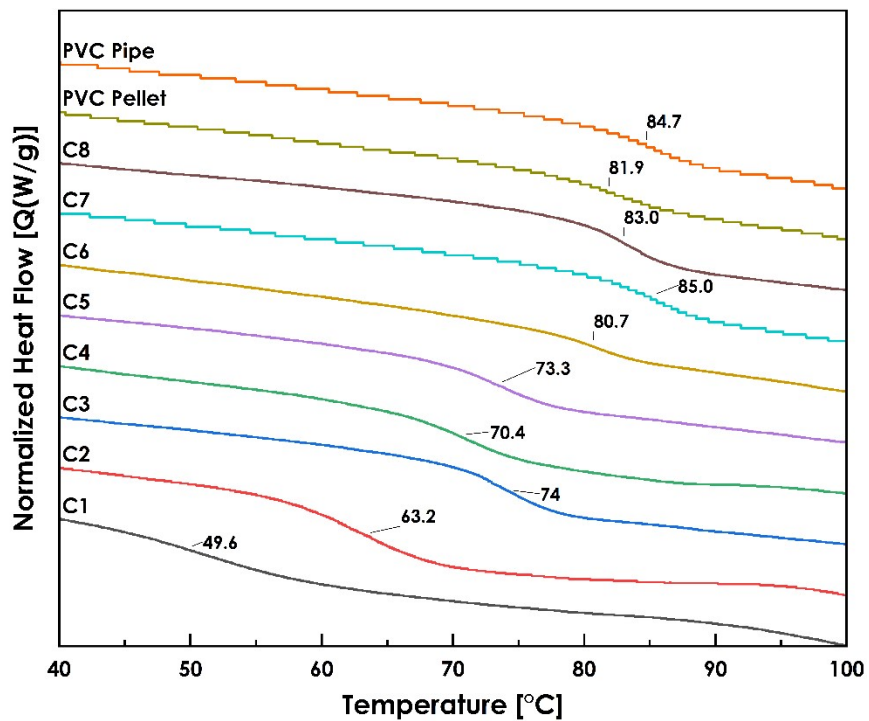


Fig. S 15 DSC scans of commercial PVC sequential fractionation products.

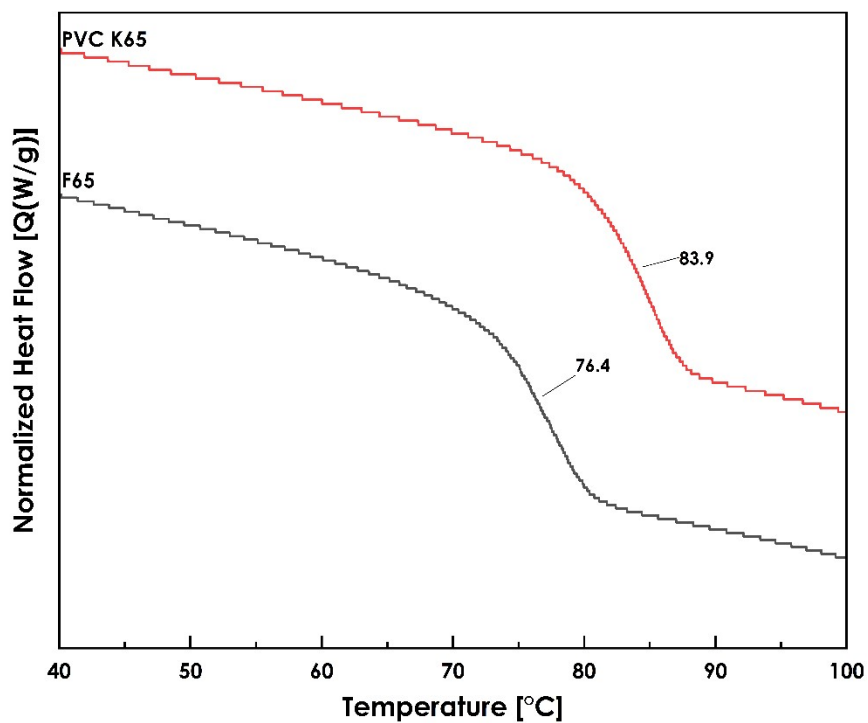


Fig. S 16 DSC scans of PVC K-65, and the product of single-step 100% Ace fractionation (F65).

S7. Other.

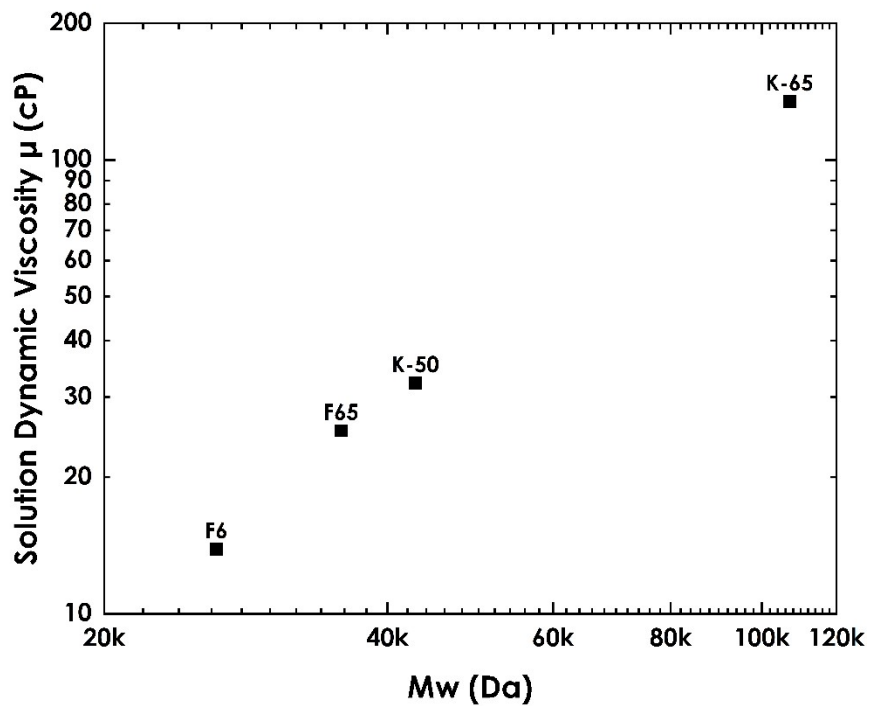


Fig. S 17 Solution dynamic viscosity ( $\mu$ ) of acetone fractions of PVC K-50 and K-65. Solution concentration: 100 mg PVC per 1 mL solvent (THF).

**Table S 4.** Summary of single-step fractionation experiments of blended PVC resins.

<b>Blend</b>	<b>Solvent System</b>	<b><math>M_w</math> (kDa)</b>	<b><math>M_n</math> (kDa)</b>	<b><math>\bar{D}</math></b>	<b>Yields (%)</b>
50% K-50 – 50% K-65	100% Ace	31.9	20.9	1.52	27.2
80% K-50 – 20% K-65	100% Ace	29.9	17.9	1.67	29.9
20% K-50 – 80% K-65	100% Ace	38.0	20.6	1.85	15.4

**Table S 5.** Summary of blended PVC molecular weight data.

<b>Blend</b>	<b><math>M_w</math> (kDa)</b>	<b><math>M_n</math> (kDa)</b>	<b><math>\bar{D}</math></b>
50% K-50 – 50% K-65	93.0	40.2	2.31
80% K-50 – 20% K-65	66.6	30.6	2.18
20% K-50 – 80% K-65	115.8	51.9	2.23
70% C3 – 30% K-65	45.3	19.9	2.28
50% C8 – 50% K-50	94.5	52.7	1.79
50% C9 – 50% K-50	99.4	51.2	1.94

## REFERENCES FOR SUPPORTING INFORMATION

1. C. Samorì, W. Pitacco, M. Vagnoni, E. Catelli, T. Colloricchio, C. Gualandi, L. Mantovani, A. Mezzi, G. Sciutto and P. Galletti, *Resources, Conservation and Recycling*, 2023, **190**, 106832.
2. T. W. Walker, N. Frelka, Z. Shen, A. K. Chew, J. Banick, S. Grey, M. S. Kim, J. A. Dumesic, R. C. Van Lehn and G. W. Huber, *Science Advances*, 2020, **6**, eaba7599.
3. K. L. Sánchez-Rivera, P. Zhou, M. S. Kim, L. D. González Chávez, S. Grey, K. Nelson, S.-C. Wang, I. Hermans, V. M. Zavala, R. C. Van Lehn and G. W. Huber, *ChemSusChem*, 2021, **14**, 4317-4329.
4. K. L. Sánchez-Rivera, A. d. C. Munguía-López, P. Zhou, V. S. Cecon, J. Yu, K. Nelson, D. Miller, S. Grey, Z. Xu, E. Bar-Ziv, K. L. Vorst, G. W. Curtzwiler, R. C. Van Lehn, V. M. Zavala and G. W. Huber, *Resources, Conservation and Recycling*, 2023, **197**, 107086.
5. J. Yu, A. d. C. Munguía-López, V. S. Cecon, K. L. Sánchez-Rivera, K. Nelson, J. Wu, S. Kolapkar, V. M. Zavala, G. W. Curtzwiler, K. L. Vorst, E. Bar-Ziv and G. W. Huber, *Green Chemistry*, 2023, **25**, 4723-4734.
6. J. Cavalcante, R. Hardian and G. Szekely, *Sustainable Materials and Technologies*, 2022, **32**, e00448.
7. J.-M. Pin, I. Soltani, K. Negrier and P. C. Lee, *Polymers*, 2023, **15**, 4714.
8. N. D. Gil-Jasso, E. A. Giles-Mazón, G. Soriano-Giles, E. W. Reinheimer, V. Varela-Guerrero and M. F. Ballesteros-Rivas, *Fuel*, 2022, **307**, 121835.
9. L. V. García-Barrera, D. L. Ortega-Solís, G. Soriano-Giles, N. Lopez, F. Romero-Romero, E. Reinheimer, V. Varela-Guerrero and M. F. Ballesteros-Rivas, *Journal of Polymers and the Environment*, 2022, **30**, 3832-3839.
10. N. Hamidi, M. Yazdani-Pedram and N. Abdussalam, *Journal of Applied Polymer Science*, 2022, **139**, 51905.
11. S. Guclu, N. Kizildag, B. Dizman and S. Unal, *Sustainable Materials and Technologies*, 2022, **31**, e00358.
12. S. Yousef, M. Tatariants, M. Tichonovas, L. Kliucininkas, S.-I. Lukošiušė and L. Yan, *Journal of Cleaner Production*, 2020, **254**, 120078.
13. C. Gong, K. Zhang, C. Yang, J. Chen, S. Zhang and C. Yi, *Textile Research Journal*, 2021, **91**, 18-27.
14. E. Yu, K. Jan and W.-T. Chen, *ACS Sustainable Chemistry & Engineering*, 2023, **11**, 12759-12770.
15. L. Wang, Y. Liu, H. Lu and Z. Huang, *Chemosphere*, 2020, **259**, 127402.
16. G. Grause, S. Hirahashi, H. Toyoda, T. Kameda and T. Yoshioka, *Journal of Material Cycles and Waste Management*, 2017, **19**, 612-622.
17. G. A. Tribello, M. Bonomi, D. Branduardi, C. Camilloni and G. Bussi, *Computer physics communications*, 2014, **185**, 604-613.
18. F. V. Olowookere, G. D. Barbosa and C. H. Turner, *Industrial & Engineering Chemistry Research*, 2024, **63**, 1109-1121.
19. P. J. Flory, *The Journal of chemical physics*, 1942, **10**, 51-61.
20. C. Hansen, *Doctoral Dissertation*, 1967.
21. H. S. Salehi, M. Ramdin, O. A. Moulton and T. J. Vlugt, *Fluid Phase Equilibria*, 2019, **497**, 10-18.
22. F. V. Olowookere, A. Al Alshaiikh, J. E. Bara and C. H. Turner, *Molecular Simulation*, 2023, **49**, 1401-1412.
23. G. Wypych, in *PVC Formulary (Third Edition)*, ed. G. Wypych, ChemTec Publishing, Toronto Ontario, 2020, DOI: 10.1016/B978-1-927885-63-5.50007-0, pp. 95-363.
24. A. Alshaiikh, S. Ezendu, D. Ryoo, P. S. Shinde, J. L. Anderson, T. Szilvási, P. A. Rugar and J. E. Bara, *ACS Applied Polymer Materials*, 2024, **6**, 9656-9662.

